

# ANN-Based Correlations for Excess Properties to Represent Density and Viscosity of Aqueous Monoethanol Amine (MEA) Mixtures.

Sumudu S. Karunarathne<sup>1</sup> Khim Chhantyal<sup>2</sup> Lars E. Øi<sup>1</sup>

<sup>1</sup>Department of Process, Energy and Environmental Technology, University of South-Eastern Norway,  
{sumudu.karunarathne,lars.oi}@usn.no

<sup>2</sup>Sekal, Norway, kc@sekal.com

## Abstract

The applicability of Artificial Neural Networks (ANNs) to represent excess properties is discussed. The excess molar volume  $V^E$  and excess free energy of activation for viscous flow  $\Delta G^{E*}$  were calculated from measured density and viscosity at different monoethanol amine (MEA) concentrations and temperatures. Different ANNs with multiple inputs and a single hidden layer were trained, validated and tested to represent  $V^E$  and  $\Delta G^{E*}$ . Developed ANN models show good accuracies in data fitting by giving  $R^2$  as 0.99 and 0.98 for  $V^E$  and  $\Delta G^{E*}$  respectively for the test data. The calculated average absolute relative deviation (AARD) for  $V^E$  and  $\Delta G^{E*}$  are 1.5 % and 1.2 % respectively for the test data that give better predictions for the density and viscosity using a Redlich and Kister polynomial for the regression. The density and viscosity models based on ANN for  $V^E$  and  $\Delta G^{E*}$  give high accuracies, which is an advantage of many aspects in engineering applications.

*Keywords: excess properties, ANN, density, viscosity*

## 1 Introduction

Physical properties like density and viscosity of aqueous amine mixtures are useful in the design and simulation of amine-based post-combustion CO<sub>2</sub> capture processes. Density and viscosity appear in most of the correlations proposed to calculate mass transfer coefficients and interfacial area between liquid and gas phases. Various approaches have been proposed to develop correlations to represent measured density and viscosity for solvents such as pure, aqueous, and CO<sub>2</sub> loaded aqueous amine mixtures (Hartono et al. 2014; Weiland et al. 1998).

The applications of ANN (Artificial Neural Network) in post-combustion CO<sub>2</sub> capture radiates into various aspects of the field. Sipöcz et al. (2011) developed an ANN model for a CO<sub>2</sub> capture plant to evaluate the amount of CO<sub>2</sub> captures, specific duty and rich loading in the solvent through the inputs of temperature, flue gas flow rate, CO<sub>2</sub> mass fraction at the inlet flue gas, solvent lean loading, solvent circulation rate and removal efficiency. The ANN is one hidden-layer feed-forward network with a back-propagation learning algorithm.

The ANN approach has been used to represent the physicochemical properties of amine solvents for post-combustion CO<sub>2</sub> capture. Hamzehie et al. (2014) discussed the prediction of CO<sub>2</sub> solubility in aqueous amine mixtures using ANN models with two hidden layers. The inputs for the network were established as in theoretical and semi-empirical models as temperature, CO<sub>2</sub> pressure, overall solute's concentration and type of solution (apparent molecular weight). The mass transfer coefficient was predicted through an ANN model by considering various input parameters gas and liquid flow rates, CO<sub>2</sub> partial pressure, liquid concentration, cyclic capacity and physical properties such as density viscosity and diffusion coefficient of CO<sub>2</sub> as illustrated by Fu et al. (2013). Several approaches were reported in literature that describe the implementation of ANN methodology to represent physical properties like density and viscosity of aqueous amine solvents (Pouryousefi et al. 2016; Haratipour et al. 2017; Garg et al. 2015). A previous study of Karunarathne et al. (2020(a)) examined the applicability of ANNs for the predictions of density and viscosity of CO<sub>2</sub> loaded alkanolamine + H<sub>2</sub>O mixtures in which mole fractions of amines and CO<sub>2</sub> in the mixture and temperature were inputs for the model while density and viscosity were the outputs.

The excess properties like excess molar volume and excess free energy of activation for viscous flow can be fitted to empirical correlations to represent density and viscosity of liquid mixtures. This work presents ANN-based correlations for excess properties to represent the density and viscosity of aqueous monoethanol amine (MEA) mixtures. The accuracy of the ANN-based correlations was evaluated by comparing the predictions with measured data other empirical correlations.

## 2 Material and Method

### 2.1 Excess Properties

The excess properties for molar volume and viscosity can be calculated from measured densities and viscosities of pure and aqueous amine mixtures as shown in (1) and (2). It is possible to fit a Redlich and Kister type polynomial (Redlich and Kister 1948) as

given in (3) to represent excess molar volume and viscosity to develop correlations for the density and viscosity of aqueous amine mixtures (Han et al. 2012; Hartono et al. 2014; Karunarathne et al. 2020(b)).

$$V^E = V - \left( \sum_{i=1}^{i=2} x_i V_i \right) \quad (1)$$

$$\eta^E = \eta - \left( \sum_{i=1}^{i=2} x_i \eta_i \right) \quad (2)$$

$$Y^E = x_1 x_2 \left( \sum_{i=0}^{i=n} A_i (x_1 - x_2)^i \right) \quad (3)$$

where  $x_i$  is the mole fraction of the components in the mixture.  $V$ ,  $V_i$ , and  $V^E$  are molar volume of the mixture, molar volume of the pure components and excess molar volume of the mixture respectively.  $\eta$ ,  $\eta_i$  and  $\eta^E$  are viscosity of the mixture, viscosity of the pure components and excess viscosity of the mixture respectively.  $Y^E$  and  $A$  are excess property and coefficients respectively in the Redlich and Kister polynomial.

The excess molar volume of different aqueous MEA mixtures was calculated from measured densities as given in (4).

$$V^E = \frac{x_1 M_1 + x_2 M_2}{\rho} - \sum_{i=1}^{i=2} \frac{x_i M_i}{\rho_i} \quad (4)$$

where  $x_i$ ,  $\rho$ ,  $\rho_i$  and  $M_i$  are mole fraction of the components in the mixture, density of the mixture, density of the pure components and molecular weights of the pure components. Subscript  $i = 1$  for MEA and  $i = 2$  for H<sub>2</sub>O.

The excess molar volume  $V^E$  arises due to the intermolecular interactions between the molecules present in the mixture and size and shape of the molecules. Positive  $V^E$  reveals the presence of weak interactions or dispersion forces and negative  $V^E$  indicates the strong specific interactions between unlike molecules. Further, negative  $V^E$  also suggests that molecules are efficiently packed due to the size and shape differences among the constituent molecules (Mahajan and Mirgane 2013; Qi and Wang 2009; Letcher and Baxter 1989).

Eyring's viscosity model (5) provides a theoretical insight into the viscosity of liquid by describing the arise of fluid friction due to the molecular jump over a potential energy barrier (Bird et al. 2002; Eyring 1936). The free energy of activation for viscous flow  $\Delta G^*$  can be calculated from measured density and viscosity data.

Semi-empirical and empirical models can be proposed to fit the calculated  $\Delta G^*$ . For a binary mixture, the excess free energy of activation for viscous flow  $\Delta G^{E*}$  is described as given in (6). The sign of  $\Delta G^{E*}$  reveals the nature of intermolecular interactions among the molecules in the mixture. The positive  $\Delta G^{E*}$  indicates the presence of strong specific interactions between unlike molecules while negative  $\Delta G^{E*}$  signifies weak intermolecular interactions like dispersion forces in the mixture (Meyer et al. 1971; Kinart et al. 2002; Ćwiklińska and Kinart 2011; Aminabhavi et al. 1994).

Eyring's viscosity model was adopted to calculate the excess free energy of activation for viscous flow as shown in (6) from measured dynamic viscosities and densities at different MEA mole fractions and temperatures.

$$\eta = \frac{h N_A}{V} \exp\left(\frac{\Delta G^*}{RT}\right) \quad (5)$$

$$\frac{\Delta G^{E*}}{RT} = \ln(\eta V) - \sum_{i=1}^{i=2} x_i \ln(\eta_i V_i) \quad (6)$$

where  $\Delta G^*$ ,  $\Delta G^{E*}$ ,  $h$  and  $N_A$  are free energy of activation for viscous flow, excess free energy of activation for viscous flow, Planck's constant and Avogadro's number respectively.

## 2.2 Density and Viscosity Measurements

The density of MEA + H<sub>2</sub>O mixtures at different MEA concentrations (30-100 mass% of MEA) and temperatures (293.15 K-363.15 K) was measured using a density meter DMA 4500 from Anton Paar (Graz, Austria). The viscosity of MEA + H<sub>2</sub>O mixtures at different MEA concentrations (30-100 mass% of MEA) and temperatures (293.15 K-363.15 K) was measured using a double-gap concentric rheometer Physica MCR 101 from Anton Paar (pressure cell XL DG35.12/PR; measuring cell serial number 8046220) (Graz, Austria). The measured data with associated uncertainties for both density and viscosity measurements are discussed in Karunarathne et al. (2020(b)).

## 2.3 ANN Network Training and Activation Function

### 2.3.1 Network Training

For the ANN models, the mole fraction of the components in the mixture and temperature were considered as the inputs to the network. All the networks are comprised of one hidden layer and multiple neurons. A data set with 72 data points were divided into 70%, 15% and 15% randomly for the training, validation and testing. Data sets were then scaled in the range of (-1, 1) as shown in (7). The optimum number of neurons for the

network was decided by examining the cost function of Mean Squared Error (MSE) as given in (8) for the learning algorithm of Bayesian Regularization (BR) for thirty neurons. The BR training algorithm regularizes ANN model parameters to reduce the complexity of the model, which helps to avoid overfitting. Figure 1 illustrates the schematic of the ANN for the excess free energy of activation for viscous flow.

$$Y = (Y_{max} - Y_{min}) \left[ \frac{X - X_{min}}{X_{max} - X_{min}} \right] + Y_{min} \quad (7)$$

where  $Y_{max}$  and  $Y_{min}$  are +1 and -1 respectively.  $X$  is the input or output variable.  $X_{max}$  and  $X_{min}$  are maximum and minimum of variable  $X$ .

$$MSE = \frac{1}{2N} \sum_{i=1}^N \left\{ (Y_i^E - Y_i^C)^2 + \lambda W^2 \right\} \quad (8)$$

where  $N$ ,  $Y_i^E$ ,  $Y_i^C$ ,  $\lambda$  and  $W$  refer to the number of data points, the measured property, calculated property, regularization parameter and weight parameter vector, respectively.

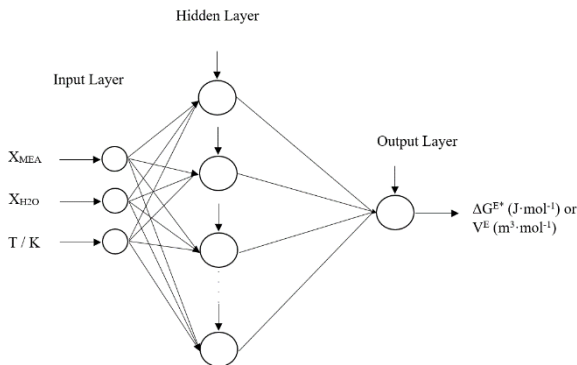


**Figure 1:** A schematic of feed forward artificial neural network with one hidden layer.

### 2.3.2 Activation Function

The input for the activation function is the sum of weighted inputs (the input from each independent variable multiplied by an adjustable connection weight) with added hidden layer bias as described in (9) (Rocabrundo-Valdés et al. 2015). For the hidden layer, the activation function is a hyperbolic tangent ( $\tau$ ) as given in (10). The output of the ANN is linearly related ( $\psi$ ) as given in (11) with the weighted output from the hidden layer and output layer bias.

$$\theta_s = IW_{(s,1)}In_1 + IW_{(s,2)}In_2 + \dots + IW_{(s,k)}In_k + b_s^{(1)} \quad (9)$$

where  $In$ ,  $\theta_s$ ,  $IW$ , and  $b_s^{(1)}$  are the inputs to the network, inputs to the hidden neurons, weight between network input and the hidden neurons and bias term to hidden neurons, respectively. The subscript  $s$  and  $k$  are for number of hidden neurons and number of inputs, respectively.

$$f = \tau(\theta_s) = \frac{2}{1 + \exp(-2\theta_s)} - 1 \quad (10)$$

$$g = \psi(LW \cdot f + b^{(2)}) \quad (11)$$

where  $LW$  and  $b^{(2)}$  are the input weights and bias in the output layer, respectively.

The ANN-based models were evaluated using average absolute relative deviation (AARD) as given in (12).

$$AARD (\%) = \frac{100\%}{N} \sum_{i=1}^N \left| \frac{Y_i^E - Y_i^C}{Y_i^E} \right| \quad (12)$$

where  $N$ ,  $Y_i^E$  and  $Y_i^C$  refer to the number of data points, the measured property and calculated property, respectively.

## 3 Results and Discussion

This section discusses the performance of ANN in excess molar volume  $V^E$  and excess free energy of activation for viscous flow  $\Delta G^{E*}$  predictions for the considered MEA + H<sub>2</sub>O mixtures.

### 3.1 Excess Molar Volume ( $V^E$ ) From ANN Based Models

The calculated  $V^E$  from (4) was used for the train, validate and test a feed forward back propagation ANN. For the MEA + H<sub>2</sub>O mixtures,  $V^E < 0$  for the considered MEA concentrations and temperatures (Karunaratne et al. 2020(b)). The accuracy of model prediction was analyzed through calculated AARD between calculated  $V^E$  and ANN is given in Table 1 for the training, validation and test data sets. Simulation provided a minimum MSE at 25 neurons. The optimum number of neurons of the network was chosen as 7 since it gives a reasonable low value for the MSE of calculated over 30 neurons in the hidden layer. Figures 2 and 3 illustrate the accuracy of the fit between ANN predictions and the calculated  $V^E$ . According to Figure 2,  $V^E$  calculated from measured properties are fitted with good accuracy into the ANN. Most of the deviation of the ANN predictions for  $V^E$  is within 2% and only one data point reported a deviation close to 6% as

illustrated in Figure 3. The developed Redlich and Kister type polynomial was able to fit data with an accuracy of 2.47% AARD and it is higher than 1.5%, which is from the ANN model for the test data set as given in Table 1. A comparison of AARD from ANN models and Redlich and Kister type polynomials for excess properties are given in Table 2. This indicates that the ANN model has a better fit for  $V^E$ .

### 3.2 Excess Free Energy of Activation for Viscous Flow $\Delta G^{E*}$ From ANN Based Models

For the  $\Delta G^{E*}$ , calculated property from (6) was used for the train, validate and test a feed forward back propagation ANN. The  $\Delta G^{E*} > 0$  for the MEA + H<sub>2</sub>O mixtures at considered MEA concentrations and

temperatures. The minimum MSE was found with 26 neurons in the hidden layer and the optimum number of neurons was considered as 7 that gives a reasonable  $R^2$  and AARD in the data fit. Equation (12) was adopted to calculate AARD to analyze accuracy between calculated  $\Delta G^{E*}$  from (6) and ANN. Table 1 summarized the  $R^2$  and AARD for different data sets reported in Table 1. Figures 4 and 5 show how good the fitting for  $\Delta G^{E*}$  between predictions from the ANN model and calculation from measured properties. Figure 5 shows that the majority of the data are within a deviation of 3% and only three data points are beyond this limit. The Redlich and Kister type polynomial for  $\Delta G^{E*}$  was able to fit data with 1.9% AARD, which indicates that the developed ANN model gives a better fit for the data.

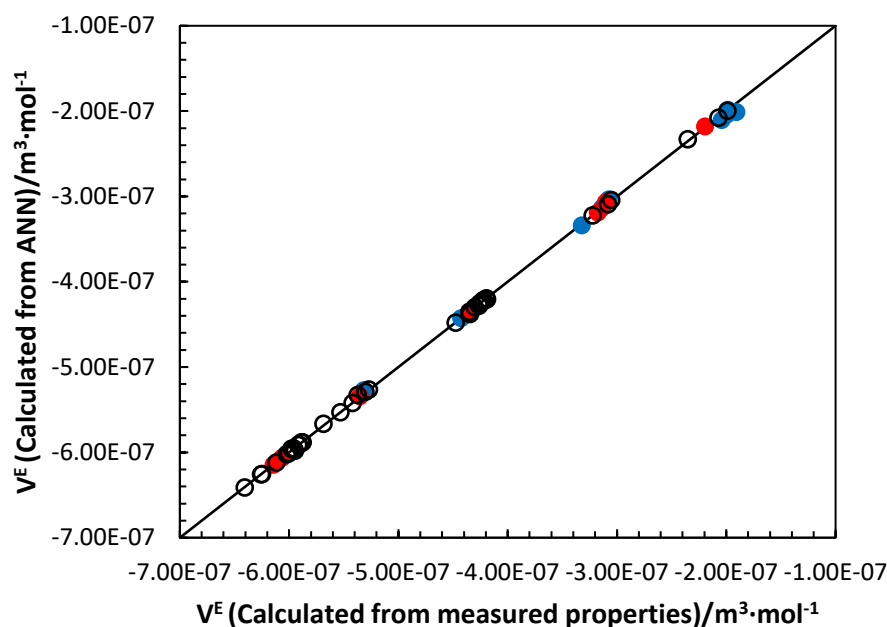


**Figure 2.** Comparison of correlated  $V^E$  with calculated  $V^E$  for MEA + H<sub>2</sub>O mixtures. ANN: Training data, ‘○’; Validation data, ‘●’; Test data, ‘●’.

**Table 1.** Performance of trained ANNs for  $V^E$  and  $\Delta G^{E*}$ .

Excess Property	No. of Neurons in the Hidden Layer	Training Data		Validation Data		Test Data	
		AARD%	$R^2$	AARD%	$R^2$	AARD%	$R^2$
$V^E$ ( $\text{m}^3 \cdot \text{mol}^{-1}$ )	7	0.2	0.999	0.4	0.999	1.5	0.999
$\Delta G^{E*}$ ( $\text{J} \cdot \text{mol}^{-1}$ )	7	0.5	0.999	0.8	0.999	1.2	0.988

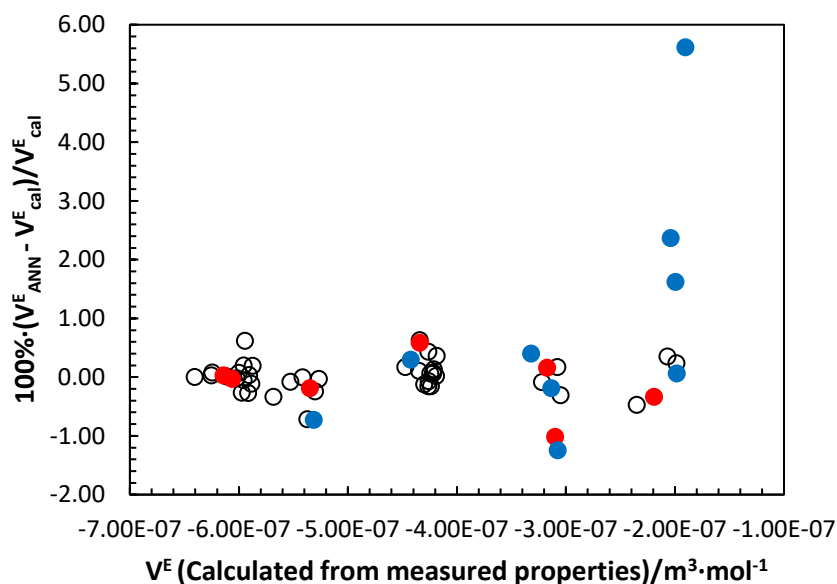


**Figure 3.** Percentage deviation of correlated  $V^E$  from calculated  $V^E$  for MEA + H<sub>2</sub>O mixtures. ANN: Training data, ‘○’; Validation data, ‘●’; Test data, ‘●’.

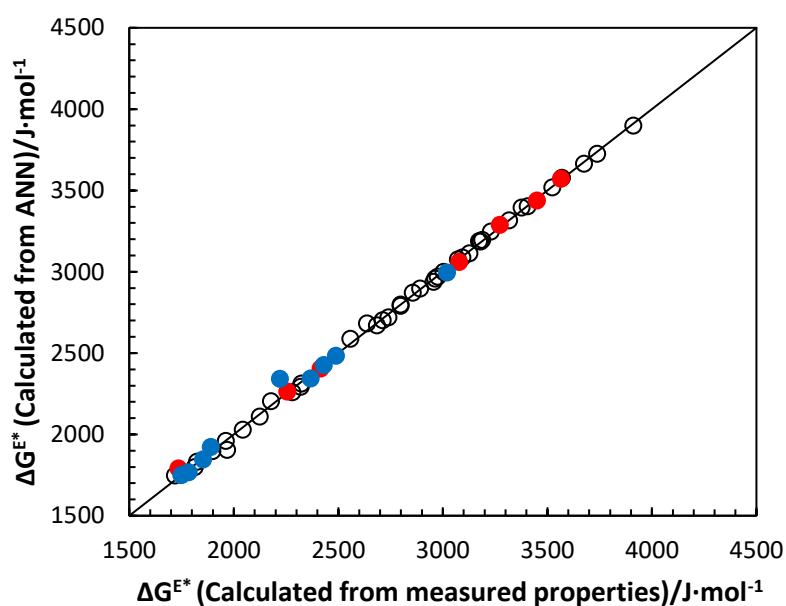


**Figure 4.** Comparison of correlated  $\Delta G^{E*}$  with calculated  $\Delta G^{E*}$  for MEA + H<sub>2</sub>O mixtures. ANN: Training data, ‘○’; Validation data, ‘●’; Test data, ‘●’.

**Table 2.** Accuracies of the data fitting for  $V^E$  and  $\Delta G^{E*}$  from ANN models and Redlich and Kister type polynomials.

<i>Excess Property</i>	<i>AARD%</i>	
	ANN	Redlich and Kister
$V^E$ (m <sup>3</sup> ·mol <sup>-1</sup> )	1.5	2.47
$\Delta G^{E*}$ (J·mol <sup>-1</sup> )	1.2	1.9

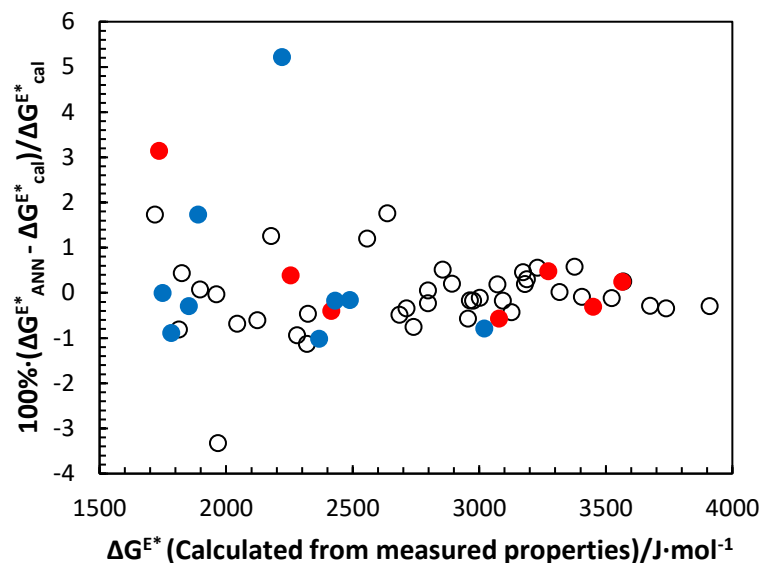


**Figure 5.** Percentage deviation of correlated  $\Delta G^{E*}$  from calculated  $\Delta G^{E*}$  for MEA + H<sub>2</sub>O mixtures. ANN: Training data, '○'; Validation data, '●'; Test data, '●'.

Literature provides accuracies for the density and viscosity correlations based on Redlich and Kister polynomial. Han et al. (2012) discussed a density correlation based on Redlich and Kister type polynomial for MEA + H<sub>2</sub>O mixtures at different MEA concentrations and temperatures. The correlation was able to represent measured density with an accuracy of AARD 0.042 %. Hartono et al. (2014) used a simplified Redlich and Kister type polynomial for both density and viscosity of MEA + H<sub>2</sub>O mixtures at different MEA concentrations and temperatures. Hartono's correlations were able to fit measured data with an accuracy of AARD 0.036 % and 3.5 % for density and viscosity respectively. The developed ANN models in this study for  $V^E$  and  $\Delta G^{E*}$  were used to calculate density and viscosity from (4) and (6). The calculated physical properties show a good accuracy compared to the measured data with AARD 0.018 % and 0.6 % for density and viscosity that is better than the correlations reported based on Redlich and Kister type polynomials in literature.

## 4 Conclusion

The excess properties of excess molar property and excess free energy of activation for viscous flows were determined from measured densities and viscosities for MEA + H<sub>2</sub>O mixtures at different MEA concentrations and temperatures. ANN models were trained to fit calculated excess properties and used to predict density and viscosity of the mixtures.

The proposed ANN model for the excess molar volume  $V^E$  was able to fit the data with acceptable accuracy. The calculated AARDs for different data sets of training, validation and test are 0.2, 0.4 and 1.5 %

respectively. The ANN model proposed for the excess free energy of activation for viscous flow  $\Delta G^{E*}$  showed AARDs for different data sets of training, validation and test are 0.5, 0.8 and 1.2 % respectively.

The models were used to predict density and viscosity at different MEA concentrations and temperatures. Results showed a good agreement with measured densities and viscosities. The accuracy for density prediction was 0.018 % AARD and for prediction of viscosity 0.06 % AARD that is higher than the accuracies based on Redlich and Kister polynomials. Accordingly, ANN approach to predict excess properties and physical properties could be used to enhance the accuracy of data fitting. The developed models are useful in the design of process equipment and process modelling for the CO<sub>2</sub> capture processes. Further, this approach can be extended to the mixtures with more than two components.

## References

- T. M. Aminabhavi, M. I. Aralaguppi, G. Bindu, and R. S. Khinnavar. Densities, shear viscosities, refractive indices, and speeds of sound of Bis(2-methoxyethyl) Ether with Hexane, Heptane, Octane, and 2,2,4-Trimethylpentane in the temperature interval 298.15-318.15 K, *J. Chem. Eng. Data*, 39: 522-528, 1994.
- R. B. Bird, W. E. Stewart, and E. N. Lightfoot. 2002. *Transport Phenomena* (John Wiley & Sons, Inc.: USA).
- A. Ćwiklińska, and C. M. Kinart. Thermodynamic and physicochemical properties of binary mixtures of nitromethane with {2-methoxyethanol+2-butoxyethanol} systems at T=(293.15, 298.15, 303.15, 308.15, and 313.15)K, *J. Chem. Thermodyn.*, 43: 420-429, 2011.
- H. Eyring. Viscosity, Plasticity, and Diffusion as example of absolute reaction rates, *J. Chem. Phys.*, 4: 283-291, 1936.

- K. Fu, G. Chen, T. Sema, X. Zhang, Z. Liang, R. Idem, and P. Tontiwachwuthikul. Experimental study on mass transfer and prediction using artificial neural network for CO<sub>2</sub> absorption into aqueous DETA, *Chem. Eng. Sci.*, 100: 195-202, 2013.
- S. Garg, A. M. Shariff, M. S. Shaikh, B. Lal, A. Aftab, and N. Faiqa. A neural network approach to predict the density of aqueous MEA solution, *Australian Journal of Basic and Applied Sciences*, 9: 415-422, 2015.
- M. E. Hamzehie, S. Mazinani, F. Davardoost, A. Mokhtare, H. Najibi, B. Van der Bruggen, and S. Darvishmanesh. Developing a feed forward multilayer neural network model for prediction of CO<sub>2</sub> solubility in blended aqueous amine solutions, *Journal of Natural Gas Science and Engineering*, 21: 19-25, 2014.
- J. Han, J. Jin, D. A. Eimer, and M. C. Melaaen. Density of water (1) + Monoethanolamine (2) + CO<sub>2</sub> (3) from (298.15 to 413.15) K and surface tension of water (1) + Monoethanolamine (2) from (303.15 to 333.15) K, *J. Chem. Eng. Data*, 57: 1095-1103, 2012.
- P. Haratipour, A. Baghban, A. H. Mohammadi, S. H. H. Nazhad, and A. Bahadori. On the estimation of viscosities and densities of CO<sub>2</sub>-loaded MDEA, MDEA+AMP, MDEA+DIPA, MDEA+MEA, and MDEA+DEA aqueous solutions, *J. Mol. Liq.*, 242: 146-159, 2017.
- A. Hartono, E. O. Mba, and H. F. Svendsen. Physical properties of partially CO<sub>2</sub> loaded aqueous monoethanolamine (MEA), *J. Chem. Eng. Data* 59: 1808-1816, 2014.
- S. S. Karunarathne, K. Chhantyal, D. A. Eimer, and L. E. Øi. Artificial neural networks (ANNs) for density and viscosity predictions of CO<sub>2</sub> loaded alkanolamine + H<sub>2</sub>O mixtures, *ChemEngineering*, 2020.
- S. S. Karunarathne, D. A. Eimer, and L. E. Øi. Density, viscosity and free energy of activation for viscous flow of monoethanol amine (1) + H<sub>2</sub>O (2) + CO<sub>2</sub> (3) mixtures, *Fluids*, 5,13, 2020.
- C. M. Kinart, W. J. Kinart, and A. Ćwiklińska. 2-Methoxyethanol–Tetrahydrofuran–binary liquid system. Viscosities, densities, excess molar volumes and excess Gibbs activation energies of viscous flow at various temperatures, *J. Therm. Anal. Calorim.*, 68: 307-317, 2002.
- T. M. Letcher, and R. C. Baxter. Application of the Prigogine-Flory-Patterson theory part I. Mixtures of n-alkanes with bicyclic compounds, benzene, cyclohexane and n-hexane, *J. Solution Chem.*, 18: 65-80, 1989.
- A. R. Mahajan, and S. R. Mirgane. Excess molar volumes and viscosities for the binary mixtures of n-Octane, n-Decane, n-Dodecane, and n-Tetradecane with Octan-2-ol at 298.15 K, *Journal of Thermodynamics*, 2013: 1-11, 2013.
- R. Meyer, M. Meyer, J. Metzger, and A. Peneloux. Thermodynamic and physicochemical properties of binary solvent *Journal de Chimie Physique et de Physico-Chimie Biologique*, 68: 406-412, 1971.
- F. Pouryousefi, R. Idem, T. Supap, and P. Tontiwachwuthikul. Artificial Neural Networks for Accurate Prediction of Physical Properties of Aqueous Quaternary Systems of Carbon Dioxide (CO<sub>2</sub>)-Loaded 4-(Diethylamino)-2-butanol and Methyl-diethanolamine Blended with Monoethanolamine, *Ind. Eng. Chem. Res.*, 55: 11614-11621, 2016.
- F. Qi, and H. Wang. Application of Prigogine–Flory–Patterson theory to excess molar volume of mixtures of 1-butyl-3-methylimidazolium ionic liquids with N-methyl-2-pyrrolidinone, *J. Chem. Thermodyn.*, 41: 265-272, 2009.
- O. Redlich, and A. T. Kister. Algebraic representation of thermodynamic properties and the classification of solutions, *Ind. Eng. Chem.*, 40: 345-348, 1948.
- C. I. Rocabrano-Valdés, L. F. Ramírez-Verduzco, and J. A. Hernández. Artificial neural network models to predict density, dynamic viscosity, and cetane number of biodiesel, *Fuel*, 147: 9-17, 2015.
- N. Sipöcz, F. A. Tobiesen, and M. Assadi. The use of Artificial Neural Network models for CO<sub>2</sub> capture plants, *Appl. Energy*, 88: 2368-2376, 2011.
- R. H. Weiland, J. C. Dingman, D. B. Cronin, and G. J. Browning. Density and viscosity of some partially carbonated aqueous alkanolamine solutions and their blends, *J. Chem. Eng. Data*, 43: 378-382, 1998.